Available online at www.sciencedirect.com
ScienceDirect
Journal of Power Sources 178 (2008) 103–117
JOURNAL OF POWER SOURCES
www.elsevier.com/locate/jpowsour

Review

A review of water flooding issues in the proton exchange membrane fuel cell

Hui Li [a], Yanghua Tang [a], Zhenwei Wang [a], Zheng Shi [a], Shaohong Wu [a], Datong Song [a], Jianlu Zhang [a], Khalid Fatih [a], Jiujun Zhang [a,*], Haijiang Wang [a], Zhongsheng Liu [a], Rami Abouatallah [b], Antonio Mazza [b,c]

[a] *Institute for Fuel Cell Innovation, National Research Council Canada, Vancouver, BC, Canada V6T 1Z4*
[b] *Hydrogenics, Mississauga, ON, Canada L5R 1B8*
[c] *School of Energy Systems and Nuclear Science, The University of Ontario Institute of Technology (UOIT), Oshawa, ON, Canada L1H 7K4*

Received 15 November 2007; received in revised form 12 December 2007; accepted 12 December 2007
Available online 27 December 2007

Abstract

We have reviewed more than 100 references that are related to water management in proton exchange membrane (PEM) fuel cells, with a particular focus on the issue of water flooding, its diagnosis and mitigation. It was found that extensive work has been carried out on the issues of flooding during the last two decades, including prediction through numerical modeling, detection by experimental measurements, and mitigation through the design of cell components and manipulating the operating conditions. Two classes of strategies to mitigate flooding have been developed. The first is based on system design and engineering, which is often accompanied by significant parasitic power loss. The second class is based on membrane electrode assembly (MEA) design and engineering, and involves modifying the material and structural properties of the gas diffusion layer (GDL), cathode catalyst layer (CCL) and membrane to function in the presence of liquid water. In this review, several insightful directions are also suggested for future investigation.

Keywords: Proton exchange membrane (PEM) fuel cell; Water management; Water flooding; Gas diffusion layer (GDL); Cathode catalyst layer (CCL); Bipolar flow field plate

Contents

* Corresponding author. Tel.: +1 604 221 3087; fax: +1 604 221 3001.
E-mail address: jiujun.zhang@nrc.gc.ca (J. Zhang).

0378-7753/$ – see front matter.
doi:10.1016/j.jpowsour.2007.12.068

1. Introduction

As environmental concerns grow and fossil fuel reserves are being depleted, hydrogen and bio-fuels have been considered as feasible and sustainable clean energy carriers for the future. Together with these carriers, fuel cells have attracted increasing attention as the most promising energy converters, due to their high-energy efficiency and low/zero emissions. Of the different types of fuel cells, PEM fuel cells are the most promising candidates, especially for automobile applications, because of their high-energy density at low operating temperatures, quick start-up, zero emissions and system robustness [1–4]. However, despite the great advances in PEM fuel cell technology over the past two decades through intensive research and development activities, the large-scale commercialization of PEM fuel cells is still hampered by the high cost of materials (such as ionomer materials and platinum-based catalysts) and low reliability (in terms of early failure modes and relatively short durability). Currently, active research is underway with the goal to reduce the cost by: (i) reducing the loading of platinum catalyst, (ii) seeking inexpensive materials and construction methods, and (iii) improving cell performance and durability [5,6].

Improvements to fuel cell performance will have far-reaching positive consequences for every aspect of fuel cell technology. It has long been recognized that, for PEM fuel cells, cathode performance [6,7] is one of the key factors affecting fuel cell performance. Two major issues contribute to the cathode being the limiting factor of the cell performance. One is the slow kinetics of the oxygen reduction reaction (ORR) at the cathode when compared to that of the hydrogen oxidation reaction at the anode. Despite improvements in catalyst formulations, the rate of ORR is four to six orders of magnitude lower than that of the hydrogen oxidation reaction [8], thus making the cathode reaction the rate limiting step. The second issue is that of the mass transport limitation imposed by liquid water, especially at high current densities. It is often difficult to remove the product water from the cathode side of the fuel cell, which leads to the compromised transferal of oxygen to the reaction sites at the cathode electrode.

The accumulation of liquid water is the major cause of the oxygen mass transport limitation in a PEM fuel cell. Water is generated in the cathode by the ORR ($O_2 + 4H^+ + 4e^- \rightarrow 2H_2O$) in addition to being transported with the proton as it travels across the electrolyte from the anode to the cathode by electro-osmotic drag. If the water removal rate does not keep up with the generation rate (at the cathode in particular), excessive water will accumulate, causing water flooding and thus hindering the transport of oxygen by blocking the pores in the porous CCL and GDL, covering up active sites in the catalyst layer and plugging the gas transport channels in the flow field. In addition, water flooding within the catalyst layer, GDL and/or gas flow channels can result in a non-uniform distribution of reactants over the active catalyst area and among cells in the stack. This non-uniformity of distribution can result in both poor performance and cell-to-cell performance variation within a stack [9,10]. Therefore, water flooding will make the cell performance unpredictable, unreliable and unrepeatable under nominally identical operating conditions [11–13].

The ionic conductivity of the proton-conducting membrane is strongly dependant on its degree of humidification, or water content, with high ionic conductivities at maximum humidification. When the water removal rate exceeds the water generation rate, membrane dehydration occurs, which can result in performance degradation due to significant ohmic losses within the cell [14]. Therefore, maintaining the proper balance in the fuel cell between water production and removal is essential in optimizing PEM fuel cell performance.

Water flooding is the most important aspect of water management, along with membrane dehydration and feed gas humidification. Water flooding, as a significantly negative factor in PEM fuel cells, is an interrelated and complex phenomenon that has garnered a significant amount of attention. Studies on the water flooding phenomena have ranged from numerical simulation and prediction (modeling), to experimental investigation and diagnosis, with the ultimate goal of developing mitigation strategies. Fundamental modeling that addresses water flooding through two-phase flow has developed rapidly, and has been useful in understanding both the importance of water management and the sensitivity of water flooding to changes in operating conditions and fuel cell components. Direct visualization and pressure drop measurement experimental methods are well developed, especially for qualitatively investigating water flooding. Efforts to mitigate flooding involve the hydrophobic

treatment of GDL with PTFE, the addition of a micro-porous layer (MPL) in the MEA, and the serpentine layout of flow field design. Each of these strategies has been very successful at flooding mitigation in a PEM fuel cell.

The purpose of this review is to summarize the progress and status of water-flooding-related research for PEM fuel cells. Firstly, the water movement and balance in a PEM fuel cell are introduced and explained briefly. Secondly, the effects of GDL, CCL, flow field and operating conditions on water flooding and cell performance are summarized. Thirdly, experimental diagnostic tools and mitigating strategies for water flooding are reviewed. Suggested research directions are also discussed.

2. Water movement inside a PEM fuel cell

Water management has a significant impact on the overall system performance, and is, therefore, one of the most critical and widely studied issues in PEM fuel cells. Proper water management requires meeting two conflicting needs: adequate membrane hydration and avoidance of water flooding in the catalyst layer and/or GDL. To ensure a fully hydrated membrane, fuel and oxidant (air) streams are fully or partially humidified before entering the fuel cell. However, under certain operating conditions, and especially at low temperatures, high humidification levels, and high current densities, the gases inside the fuel cell become oversaturated with water vapour and condensation may occur at the cathode side, resulting in reduced performance. Clearly, adequate understanding of water generation, transport and distribution within the PEM fuel cell is essential.

Fig. 1 schematically depicts water transport in a PEM fuel cell [4,14–17]. Water is generated internally at the cathode catalyst–membrane interface as a result of ORR, and is also supplied to the fuel cell by humidified reactant gases or by direct liquid hydration [18,19], represented by anode and cathode inlet relative humidity values. Through the membrane between the anode and the cathode, two modes of water transport occur: electro-osmotic drag transport and back-diffusion transport. The former drives the water migration from the anode to the cathode along with the protons, and the latter, caused by the concentration gradient of water across the membrane, drives the water flux towards the anode. The water flux due to the electro-osmotic drag effect is proportional to the protonic flux (I_{cell}/F), and the back-diffusion flux is related to the water diffusion coefficient through the ionomer and the concentration gradient of water. In addition, a sufficient amount of water that is generated at the cathode must be transported away from the catalyst layer by evaporation, water–vapor diffusion and capillary transport of liquid water through the GDL into the flow channels of the flow field, and then exhausted at the outlet. If this does not occur, excess water exists at the cathode side and condenses, thus blocking the pores of the GDL and reducing the active sites of the CCL. This phenomenon is known as "flooding", and is an important limiting factor of PEM fuel cell performance. The extent of flooding and the effects of flooding depend upon the interaction of the operating conditions and the MEA properties. Generally, flooding of an electrode is linked to high current density operation that results in a water production rate that is higher than the removal rate. However, flooding can also occur even at low current densities under certain operating conditions, such as low temperatures and low gas flow rates, where faster saturation of the gas phase by water–vapor [20] can occur. Therefore, water management is a critical design consideration for PEM fuel cell systems. The amount and disposition of water within the fuel cell strongly affects efficiency and reliability [21].

3. PEM fuel cell water flooding and its effects on cell performance

As discussed above, excess water in a PEM fuel cell can cause water flooding, resulting in a significant loss of cell performance. In Fig. 2, polarization curves with various degrees of water flooding are compared to a curve that is free from flooding. It can be seen that the slopes of the cell performance curves affected by water flooding become much steeper at the higher current densities where internal water production is greater. This significant performance loss is attributable to the greatly reduced oxygen transport rate incurred by water flooding at high current densities where the water generation rate exceeds the water removal rate.

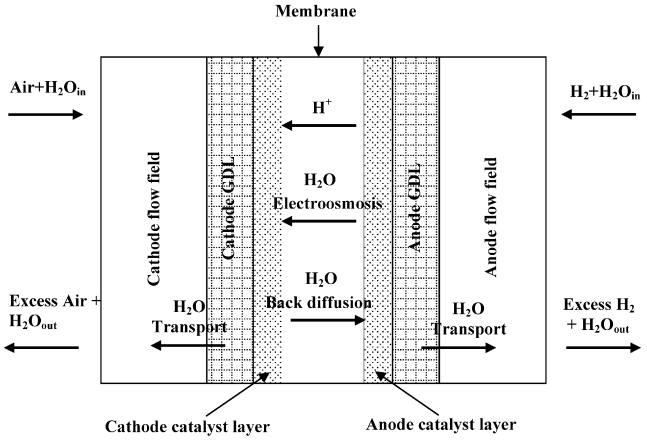

Fig. 1. Schematic picture of water movement inside a PEM fuel cell.

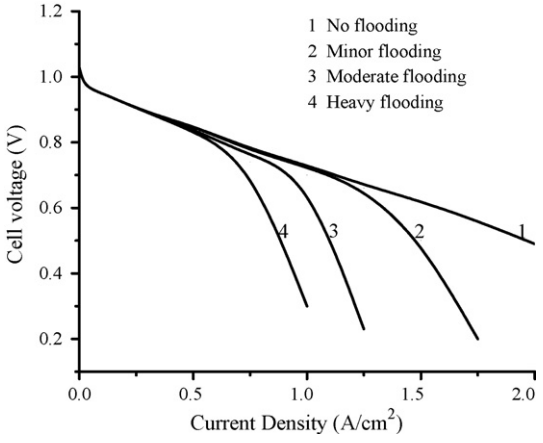

Fig. 2. Polarization curves of a PEM fuel cell illustrating the effect of water flooding on cell performance: (1) no flooding; (2–4) increasing water flooding.

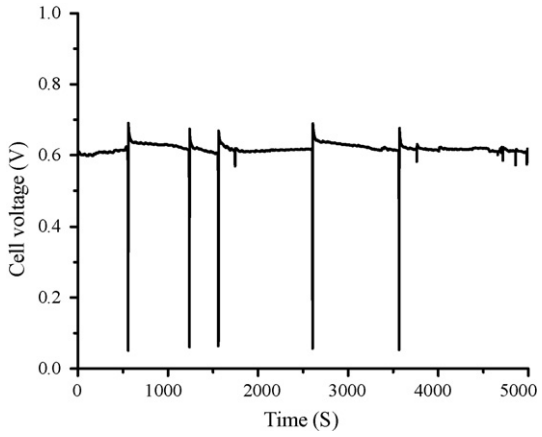

Fig. 3. A typical water flooding pattern in a PEM fuel cell operated at constant current density.

The time-dependent oscillation of cell voltage at fixed current density shown in Fig. 3 represents a typical flooding pattern in a PEM fuel cell (as observed in the NRC/IFCI laboratory). When the operating conditions allow the liquid water to accumulate to some extent and severe water flooding occurs, the gas flow path can be temporarily blocked, giving rise to a negative spike in cell voltage; then the blocking of the gas flow path can result in a sudden build-up of local pressure that quickly flushes out the excess liquid water, thereby resulting in a quick restoration of the cell voltage. The periodic build-up and removal of liquid water in the cell causes the observed fluctuation in the cell performance, causing unstable, unreliable and inconsistent cell performance. Of course, depending on the properties of the fuel cell components, the flooding pattern may be different from the one illustrated in Fig. 3. In addition, water flooding not only compromises the cell performance in a transitory manner but also degrades the durability of the fuel cell [11].

It has to be noted that flooding occurs not only in the GDL and/or the catalyst layer but in the gas flow channels of the flow field as well, depending on the interplay of the properties and engineering of those components, and the operating conditions. Therefore, it is important to understand how these variables affect water flooding both independently and interactively.

The general consensus is that water flooding is more prone to occur at the cathode, where water is generated by the ORR and electro-osmotic drag. Therefore, the literature has focused almost exclusively on cathode flooding, with a few exceptions [22,23]. In this review, the term "flooding" refers to "cathode flooding" unless otherwise stated.

3.1. Effects of GDL on flooding

The GDL is a key component of a PEM fuel cell that fulfills several functions [24]: (1) reactant gas permeability: providing access for reactant gases from flow-field channels to catalyst layers; (2) liquid permeability: providing paths for product water to be removed from the catalyst layer area to flow field channels; (3) electronic conductivity: providing passage for electron transport from bipolar plates to catalyst layers; (4) heat conductivity: providing efficient heat conduction between bipolar plates and MEA; and (5) mechanical strength: providing mechanical support to the MEA. These functions, especially the interfacial electrical and thermal conductivities between the bipolar plates and catalyst layers, depend significantly on the GDL compression behavior. Porous carbon materials, such as carbon paper and carbon cloth, are the most commonly used materials for GDLs [25–29]. Mathias et al. [24] present detailed information on the different materials and manufacturing procedures of GDLs.

The GDL plays a crucial role in water management that maintains the delicate balance between membrane hydration and water removal. Product water must be transported through the GDL from the catalyst layers to the flow field channels. If the liquid water accumulates in a region needed for reactant supply, flooding will occur and significant gas transport limitations can result. To avoid flooding the porous interstitial spaces with accumulated water, the GDL is often treated with hydrophobic materials, such as PTFE, to change its wetting characteristics so that the water is better expelled. Such treatment results in hydrophobic and hydrophilic pockets of pores in the GDL [24,30,31], which allow separate paths for gas transport and liquid water transport [32–38]. Various techniques have been developed to load the PTFE into the GDL, such as dipping, spraying and brushing. A wide range of PTFE loading has been used, generally falling between 5 and 30 wt.%.

In addition to the bulk hydrophobic treatment of the GDL, a micro-porous layer (MPL) is often added between the GDL and the catalyst layer to: assist in the distribution of the reactant gas flows to the catalyst surface; enhance the mechanical compatibility and contact between the layers; improve the local current density distribution; and most importantly, provide effective wicking of liquid water from the catalyst layer into the GDL [24]. To distinguish a MPL from a GDL, this paper defines a GDL as the combination of a gas diffusion media (GDM) and a MPL. MPLs are usually a mixture of carbon or graphite particles and a polymeric binder (usually PTFE), coated on one side of the GDM [39]. It is an industrial practice to refer to this MPL as a carbon sub-layer. The pore size of MPLs ranges from 0.1 to 0.5 μm compared with 10 to 30 μm for GDMs [24].

Water transport in the GDL is a complex process due to the two-phase flow conditions. The two-phase flow in the porous GDL is governed by capillary force, shear force and evaporation, and the relative magnitudes of these forces control the two-phase distribution and flow regimes [32,40]. Within the cathode side GDL of a PEM fuel cell, most of the product water moves in the direction of the flow channel by gas-phase diffusion and/or liquid-phase transport. When humid air is introduced into the cathode compartment, the water vapor generated from ORR may partially or completely condense.

Among the properties that the GDL must possess to fulfill the multi-functionality listed above, several of them are related to water management, including porosity, wettability (contact angle), pore size, thickness and fluid permeability (fluid transport). Most of the characterization techniques of these properties are still under development. However, some techniques are presently established, such as the measurement of porosity and contact angle. The characterization of the two-phase transport properties, such as the diffusion coefficients of the gases and

the coefficients for capillary-induced liquid transport, has been the main focus of the characterization study of GDLs [41–43]. Due to the unique and important role that the GDL plays in transporting gases and water, most attention has been drawn to it in the examination of water flooding issues in PEM fuel cells. Yang and Zhang [44] carried out experimental investigations by using transparent fuel cells to probe the details of liquid water transport from the GDL into the gas flow channels. Numerical approaches have also been very important in numerous studies of the two-phase transport in GDLs [1,45–47].

3.1.1. Effects of PTFE treatment and the PTFE content of GDLs

Although PTFE treatment has become a common industrial practice in preparing GDLs, there has been much research interest in studying the effects of PTFE treatment and the PTFE content of GDLs [5,32,48–50]. Shimpalee et al. [49] experimentally and numerically studied the effects of PTFE treatment of the GDM on flooding and cell performance. In their experiments, they investigated two different types of GDM: one was PTFE-treated to create a hydrophobic surface while the other was not treated at all. The same PTFE-treated MPLs were employed in both cases to isolate the effect of the GDM from that of the MPL. Fig. 4 shows the polarization curves at the following operating conditions: 65 °C cell temperature, anode and cathode gases at 100% relative humidity (RH), 1.2/2.5 H_2/Air stoichiometries, triple serpentine flow field channels and with 0 psig back pressure. The cell performance obtained with the untreated GDM is observed to be significantly lower than that with the PTFE-treated GDM. At about 0.6 A cm^{-2}, the cell voltage is 200 mV lower with the untreated GDM, due to severe flooding in that fuel cell. They also carried out numerical modeling to predict cell performance by correlating the effective diffusivity with the degree of water flooding. Their model was based on a steady-state, multi-phase phenomena and a three-dimensional mass transfer process, including the heat transfer process in a PEM fuel cell. Their modeled cell performance was in good agreement with the experimental results for both PTFE-treated and untreated GDMs.

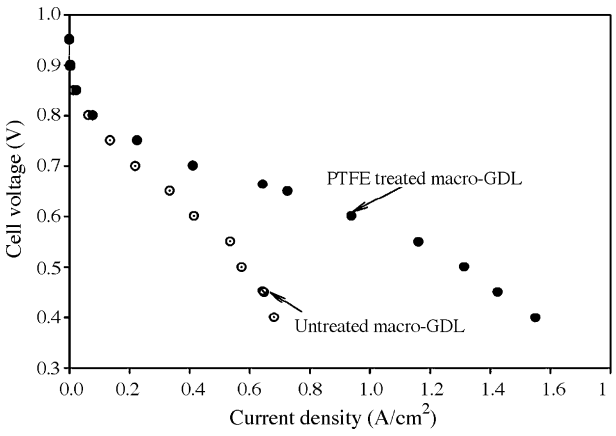

Fig. 4. Experimental data of PTFE treated and untreated GDLs under 65 °C, 40% H_2/air, 100%/100% RH, 1.2/2.5 stoichiometries, 0 psig [49] (with permission from Elsevier Ltd.).

Tüber et al. [48] experimentally studied the water flooding issue in small fuel cells for portable applications operated at ambient pressure and low temperatures (<30 °C) and in the current density range of less than 0.25 A cm^{-2}, using untreated and treated Toray paper as the GDL. They investigated the influence of the wetting properties of the GDM on water flooding and cell performance, by treating the standard Toray carbon paper (TGP-H-90) to make it strongly hydrophobic (20 wt.% PTFE). Their results suggested that the wetting property of the GDL could directly influence the accumulation of product water in the gas channels if the operating temperature was in the vicinity of 30 °C as would be the case during fuel cell start-up and outdoor operation. Specifically, the hydrophilic GDL turned out to be the more effective one in reducing water flooding, due to effective water removal from the CCL to the GDL.

The effects of PTFE content in the GDM and MPL have been widely studied [5,32,51]. Park et al. [32] studied the behavior of water in the GDM with a wide range of PTFE content (0–45 wt.%) under various single-cell operation conditions. They concluded that the capillary force in the GDM was not the main driving force for water transportation. Instead, the shear force of fluid and water evaporation were the dominant driving forces due to the relatively larger pores of the GDM compared to those of the CCL and MPL. They also concluded that the increased PTFE content in the GDM hampered the ejection of water from the catalyst layer to the flow channels through the GDM, especially at conditions with high relative humidity. This would result in water flooding of the catalyst layer. Velayutham et al. [5] experimentally investigated the effects of PTFE content in the GDM and MPL. The PTFE content ranged from 7 to 30 wt.% in the GDM and 10 to 32 wt.% in the MPL. They found that the optimal PTFE contents were 23 and 20 wt.% for the GDM and MPL, respectively, in terms of water flooding control at the operating conditions under which they carried out their study.

3.1.2. Effects of the GDL materials

Manufacturing methods and materials used can significantly affect the water management characteristics of the GDL and the performance of the cell in which it is placed [25–29,52,53]. Development and modification of GDLs to improve cell performance has been the focus of attention of many studies. Although most of the reports concluded that the enhanced fuel cell performance by modifying GDLs was the result of improved gas permeability and electrical conductivity, the role of GDLs in improving water management cannot be ignored.

There have been numerical [54–56] and experimental [36,39,50] approaches to study the effects on water management of GDLs with different materials or different properties. For example, Spernjak et al. [39] explored the influence of GDL materials on water formation and transport, using untreated carbon cloth from Ballard, untreated carbon paper from Toray and 5 wt.% PTFE-treated carbon fiber from SGL Carbon. The direct visualization technique in their experiments showed that water dynamics changed as the GDL material changed. With the PTFE-treated GDL material from SGL, water emerged as droplets over the surface of the flow channels, but with the Bal-

lard and Toray GDL materials, water tended to move along the sidewall of the channels in the form of films and slugs. Spernjak et al. believed that the water droplet removal mechanism was far more effective than the film and slug removal mechanism. Furthermore, the untreated Ballard and Toray GDLs were unable to push the water to the membrane side through the catalyst layer, just as they were not able to efficiently expel the water into the flow channels of the bipolar plates. This resulted in poor membrane hydration and thus low ionic conductivities of MEAs that were made with the Ballard and Toray GDLs. It should be pointed out that, in their experiments with the SGL material, other properties of the GDL materials, such as pore structure, average pore diameter and pore diameter distribution, thickness, tortuosity, porosity and the addition of a MPL could have played some roles in the water removal mechanism.

3.1.3. Effects of the MPL

The attention to the MPL as an additional layer to a conventional GDL for better water removal from the catalyst layer is reflected in the number of papers that have been published in recent years [16,27,30,34,39,51,54,57–67]. The consensus now is that the placement of a MPL between the GDM and the catalyst layer can greatly improve cell performance, as illustrated in Fig. 5. However, the explanation for this improvement is still a subject for debate.

Qi et al. [51] experimentally studied single-cell performance with and without a MPL. In addition to benefits in cell performance afforded by inclusion of a MPL layer, such as diminishing the differences between different GDMs, preventing the catalyst from penetrating deeply into the GDM, and making the contact between catalyst and GDL more intimate, they particularly reported the definite enhancement of fuel cell water management with the presence of a MPL. Qi et al. also speculated that the microporosity and more uniform pore distribution might be the major contributors to the improved water management, and the improved water management could make, not only the MPL itself, but also the catalyst layer less likely to be flooded.

Nam et al. [54] and Pasaogullari et al. [57] found through half-cell modeling that the placement of a MPL helps reduce water saturation in the adjacent CCL and enhances water removal rate from the CCL to the cathode GDM, thereby preventing CCL flooding. Weber et al. [58] employed a two-phase, two-dimensional fuel cell model to study the influence of the MPL on water transport. They fitted their key model parameters from the experimental data of Qi and Kaufman [51]. Based on their modeled results, they claimed that the MPL acts as a valve that forces water away from the cathode side and through the membrane to the anode side, which is in contrast to the modeled results from Nam et al. [54].

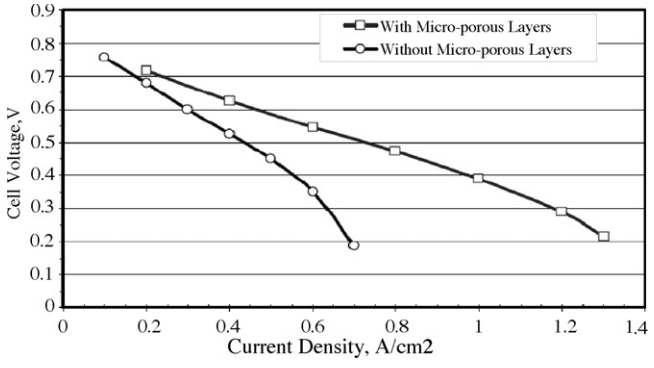

Fig. 5. Cell performance curve with and without a MPL in the MEAs (T_{cell}: 60 °C; $T_{anode\ humidifier}$: 80 °C; $T_{cathode\ humidifier}$: 30 °C; hydrogen stoich: 2.5; air stoich: 2.5) [3] (with permission from ECS—The Electrochemical Society).

Lin et al. [60] experimentally investigated the effects of different MPLs on water flooding and cell performance. From the positive effect observed by adding a MPL to the GDM, they hypothesized that the MPL increases the back-diffusion of water from the cathode through the membrane to the anode.

These studies [23,39,51,54,57–59] obviously present contrasting explanations about the role of the MPL in water transport. However, the results of later research [23,39,59] appear to agree on the role of the MPL, i.e. (1) saturated vapor pressure is higher inside the MPL than inside the GDM, due to smaller pore size and enhanced hydrophobicity, rendering the MPL less prone to flooding; (2) the MPL renders the GDL more like a pressure valve with a two-fold function: pushing the water to the membrane side to effectively hydrate the membrane, and providing a pressure buildup necessary to expel the water through the less hydrophobic GDM pores into the cathode flow channels.

In order to clarify whether the MPL enhances back-diffusion of water from the cathode to the anode, or to improve water removal from the CCL to the GDM, Atiyeh et al. [30,68] recently carried out a systematic experimental study of the net water drag under various operating conditions. Their preliminary results have shown that the function of the MPL in improving water management and fuel cell performance was not associated with overall water drag.

3.1.4. Effects of porosity

The porous structure of both the GDM and the MPL is one of the most important factors that influence the two-phase transport across the GDL. It not only determines the permeability for the gases and liquid water but also affects the liquid water saturation profile across the GDL and catalyst layer [57]. The effect of GDL porosity has been studied mostly in modeling work, in which the porosity of the GDL has often been assumed, for the sake of simplicity, to be uniform and constant during fuel cell operation [69–72,55,73]. However, this may not reflect the importance of GDL porosity for liquid water transport. Due to the complex and highly porous structure of the GDL, any change in its composition or morphology can lead to a substantial change in porosity and thus have a significant influence on cell performance [27,33,74–76]. During fuel cell operation, the presence of liquid water in the GDL can change the effective porosity and this change may vary with time and position. In their numerical studies on the effect of porosity on water flooding and cell performance, Chu et al. [33] employed the concept of "effective porosity" to account for the porosity change that was caused by liquid water accumulating in the pores of the GDL. They reported that a higher porosity in the GDL would lead to a higher consumption of oxygen. However, a high poros-

ity would be accompanied by water flooding in the GDL, which would markedly decrease the cell performance.

In summary, the effects of the GDL, including both the GDM and the MPL, on water flooding are very complex, depending on the interactions of several properties of the GDL (porosity, morphology, thickness and the PTFE content) and the interaction between the GDL and the flow fields of a PEM fuel cell [46].

3.2. Effects of flow field design on flooding

The water that is transported from the GDL to the flow channels must be removed from the flow channels to be exhausted out of the fuel cell. Therefore, water management along the gas flow channels is also important for effective water management of a PEM fuel cell. In fact, the appropriate design of flow channels has been considered to be the most successful strategy in tackling water flooding issues, among others [41,52]. Fig. 6 shows the three main flow field layouts developed so far: the conventional flow field consisting of straight parallel channels, the interdigitated flow field and the serpentine flow field.

In the conventional flow field where gases flow within parallel channels over the surface of the GDL, diffusion is the dominant mechanism for the reactants and products to travel to and from the electrode. Consequently, liquid water may accumulate and cell performance can be limited by the transport rate of the reactants. This design has been proved by many researchers to be prone to unacceptable non-uniformity in air streams and catastrophic flooding [77–79]. Therefore, this layout is only suitable for applications in which high gas flow and low-pressure drop are required [3].

The interdigitated flow field, which consists of dead-ended inlet and outlet channels, was proposed by Nguyen to resolve the water flooding issue [77]. In the interdigitated flow field, the incoming reactant gas is forced to flow through the GDL to the catalyst layer. As a result, the transport of the reactant and product to and from the catalyst layer through the GDL is changed from a diffusion dominant mechanism to a forced convection mechanism, which provides a much higher transport rate. More importantly, the shear force exerted by the gas flow flushes the liquid water out of the electrode, thus effectively reducing the water flooding of the cathode and significantly improving the cell performance [18]. However, forcing gas to flow through the GDL requires higher pressures, which can result in significant parasitic power loss. Furthermore, the highly enhanced mass transport in the GDL could lead to membrane dehydration at low current densities if a dry feed is used [3].

The serpentine flow field, including single and multiple parallel serpentine channels, is the most widely known and used, often regarded as the "industrial standard" due to the high cell performance and durability/reliability associated with this layout [41]. In a serpentine flow field, the flow is mainly along the channels. However, the contrast between the small channel cross-section, in the order of 1 mm by 1 mm or smaller, and the long length of the channels, in the order of meters, plus the numerous turns, together create a higher pressure drop between adjacent channels. This higher pressure drop promotes a cross-leakage flow between the adjacent channels and through the GDL, thus allowing the serpentine flow field design to have the convective feature of the interdigitated flow field and its inherent benefits. However, the serpentine flow field has its own drawbacks, which include significant parasitic power loss due to higher pressure drop [80,81], and a possibly significant decrease of reactant concentration along the long flow path. More importantly, the use of a serpentine flow field often causes membrane dehydration near the channel inlet region, while water flooding occurs near the channel exit due to excessive water carried out by the gas stream from upstream. This contributes to scale-up difficulties [20,41]. For a dry reactant stream or in cases where operations are at less than 100% relative humidity, a single serpentine flow field can result in a loss of cell performance at low current densities, due to membrane dehydration [82,83].

As discussed above, the layout of the flow field can have a significant effect on the water removal capability of a PEM fuel cell. However, even with the same layout of the flow field, the degree that the layout affects the water removal capability depends on the operating conditions. Therefore, it is crucial to fundamentally understand how operating conditions affect water behavior and transport of reactants in flow channels, in order to optimize the operating conditions for a specific flow field layout. There has been extensive modeling work on the serpentine flow field, describing the water transport phenomenon along the gas flow direction [84], studying the effects of vapor and liquid water on the gas concentration profile along the gas flow direction [85], simulating the liquid water profiles [45] and pressure change profiles [84,86–88] along the flow channels, and investigating the effects of operating conditions on flow chan-

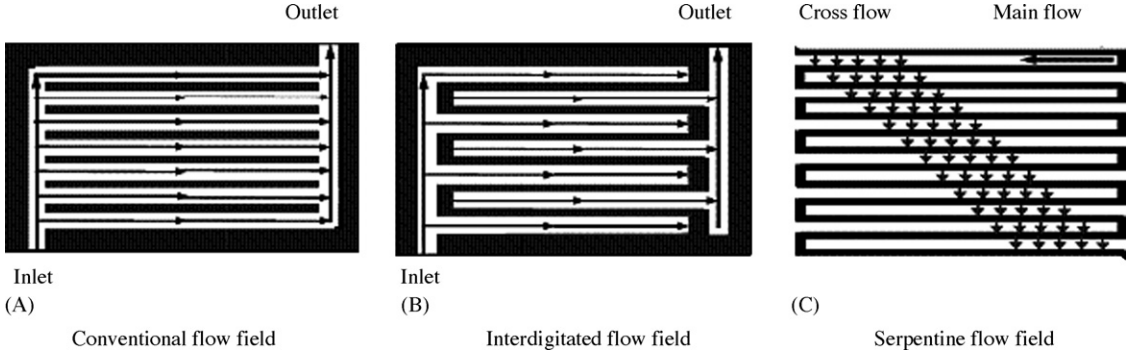

Fig. 6. Flow field designs: (1) conventional; (2) interdigitated; (3) serpentine [3] (reproduced by permission from ECS—The Electrochemical Society).

nel water flooding [18,89]. It should also be emphasized that in addition to the flow channel layout, channel dimensions [41,77] and cross-section geometry [90] also influence water removal and cell performance.

3.3. Effects of the CCL on flooding

A CCL, placed between the membrane and the GDL, consists mainly of catalyst particles, an ionomer and pore space, each of which are critical for the formation of the three-phase boundary where the ORR takes place to produce water. An insufficient amount of water in the CCL result in reduced ionic conductivity and render the catalyst surface partially accessible, which will, in turn, contribute to resistive and kinetic cell voltage loss [91]. Too much water, on the other hand, will block the catalyst surface and constrain reactant gas transport, which will lead to mass-transport-related performance loss.

Over the last few decades, research efforts on PEM fuel cell catalysts have been focused on reducing platinum loading. As a result of these efforts, the catalyst layer has developed from the conventional PTFE bonded catalyst to the thin-film Nafion bonded catalyst, with the platinum loading reduced from 4 mg cm^{-2} to as low as 0.014 mg cm^{-2} [92,93]. In addition to the work on catalyst loading, efforts have focused on optimization of the properties of the CCL, including the reactant permeability, ionic and electronic conductivity, porosity and wettability, in order to achieve higher utilization of the catalyst material.

The role of the CCL in water balance has never been explored in depth either experimentally or numerically, in contrast to the intensive research activities studying the effects of the GDL and flow fields on water management. Most cell and stack models among the published modeling work on PEM fuel cells treat CCLs as infinitesimally thin interfaces without structural resolution. Eikerling and Kornyshev [94] recently developed a structure-based model that links spatial distributions of processes across the CCL with water handling ability and cell performance. The results from the model reveal that the CCL is the prime component for the conversion of liquid water to vapor and acts like a watershed that regulates the balance between the opposing water fluxes toward the membrane and the GDL.

3.4. Effects of operating conditions on flooding

PEM fuel cell operating conditions include inlet humidity of the feed streams, cell temperature, operating current density, back pressure, air and fuel stoichiometric flows, and other factors. Favorable operating conditions can vary widely and depend on the application. For example, zero or minimal humidification combined with ambient temperature and pressure are desirable for portable devices. High relative humidity (60–100%) of the feed streams, 50–200 kPa (gauge) back pressure and operating temperatures around 80 °C are preferred for stationary and automotive applications. These operating conditions interactively affect the water balance in the fuel cell and ultimately the cell performance. However, the optimal conditions in terms of water management depend on the given membrane and electrode assembly. Typically, the effects of operating conditions on water balance and cell performance are determined through modeling for each MEA and GDL combination [2,7,21,51,95–100]. As an alternative to these theoretical methods, extensive experimental procedures can be used to quantify these effects for a specific combination of MEA and GDL [22,23,39,101]. Therefore, any conclusion about the effects of operating conditions depends on the component specifications of the fuel cell used in the work and must be validated. Generally, humidification of the feed streams ensures the hydration of the membrane, especially at low current densities. However, at higher current densities where more water is electrochemically produced, high humidification may cause excessive water accumulation that can result in water flooding. Back pressure and feed stoichiometric flow have significant influences on the pressure drop of the two-phase flow, which directly affects the movement of water in the GDL and along the flow channels and thus affects the water balance in the fuel cell. Cell operating temperature determines the water saturation level of the feed streams in the GDL and catalyst layer, which in turn affects water evaporation and condensation. Normally, as the operating temperature increases, the saturation vapor pressure increases and surface tension between water and substrate decreases, which makes liquid water evaporate more easily and thus lowers the water flooding level [102]. However, the increased water vapor pressure at high temperature may result in the reactant gas being significantly diluted [10].

To illustrate graphically the effects of operating conditions on flooding, pressure drop and cell voltage, an experimental plot from the work of Barbir et al. [103] is presented in Fig. 7 for a three-cell stack consisting of six parallel channels in a serpentine flow field layout. It can be seen that, when the humidification temperature is higher than the stack temperature, the air stream cools down and some of the water in that stream will condense. As a result, water flooding occurs, which is characterized by erratic cell potential behavior, and is also reflected in an increased pressure drop. As the stack temperature rises above the humidification temperature and water condensation slows or stops, the pressure drop starts to decline and the cell performance becomes relatively stable.

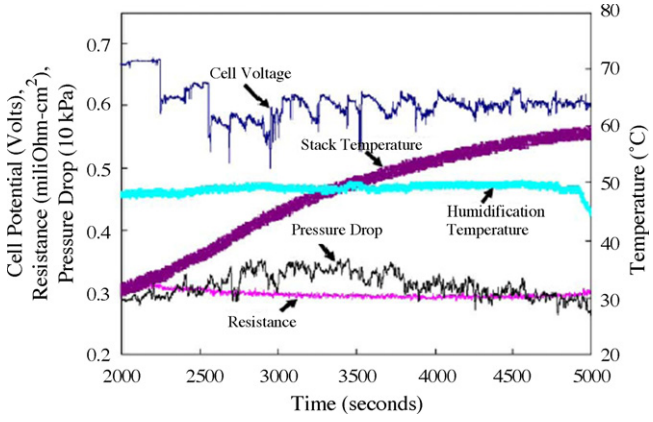

Fig. 7. Illustration of stack flooding and recovery [103] (with permission from Elsevier Ltd.).

4. Modeling work on water flooding

The number of PEM fuel cell modeling papers has been increasing dramatically over the last decade, by the dozens per year. The complexity and scope of the models have also increased. The models have evolved from the zero-dimensional or one-dimensional, single-phase flow, isothermal models that only cover some of the layers of the fuel cell sandwich [15,71], to two-dimensional or three-dimensional, non-isothermal models that involve all layers of the sandwich [7,56,85,89]. Recently, the inclusion of two-phase flow phenomena and transient phenomena is becoming more common [7,57,104,105]. Detailed consideration of water management at each region of the fuel cell has become a new trend [9,40,98]. More and more modeling work has begun to study the effects of water flooding on cell performance [7,49,95,96], or to predict water flooding of the fuel cell [96,97,106,107].

Wang [20] has provided a comprehensive review of fundamental models for PEM fuel cell engineering, and Weber et al. [108] have given a detailed overview of transport modeling in PEM fuel cells. Both these reviews cover publications through the end of 2003. More recent reviews of PEM fuel cell modeling are also available [109,110]. Therefore, a review of water management modeling is not presented in the present work.

5. Experimental diagnosis and mitigation of water flooding

Flooding is a poorly understood phenomenon. There are no established diagnostic tools at present time to identify in which part of the structure of a PEM fuel cell the flooding occurs. Furthermore, no universally applicable strategies exist for water management. This is due to the fact that water transport in various components is affected by operating conditions such as feed stream humidification levels, cell temperature, back pressure, etc. However, there has been an abundance of research attention toward the development of diagnostic tools and mitigating strategies for the issues surrounding water flooding in PEM fuel cells.

5.1. Experimental diagnosis of water flooding

Diagnostic tools for monitoring water dynamics and detecting water flooding in PEM fuel cells can be classified into two groups: imaging techniques and measurements of physical indicators.

5.1.1. Imaging techniques

Known imaging techniques for monitoring the water dynamics and water distribution inside PEM fuel cells include direct visualization [4,39,44,48,102,111], neutron imaging [112,113], magnetic resonance imaging [114,115] and X-ray imaging [116]. Among these, the direct visualization technique has been the most widely used. It requires a transparent cell plate that allows access to the channels for optical devices, including digital camcorder and high-speed camera [39,48], infrared camera [102] and CCD camera [4,117]. Direct visualization offers the advantage of studying the two-phase flow at different levels in an operating fuel cell, from the flow field level [48,102] to the smaller scale of the GDL pores [44,111] and to the micro-scale of the catalyst surface [39]. It is especially useful to directly observe the effects of operating conditions on water droplet formation, growth and movement. However, the visualization technique primarily provides qualitative data because of limited depth perception from the top of the transparent window, and also because of the highly reflective nature of GDLs, which make it almost impossible to quantitatively evaluate the volume of water [39].

Neutron imaging has been recognized by Ballard [91] as the only diagnostic tool that provides all of the three requirements for diagnostic tools in water management: in situ applicability, minimal invasiveness and the ability to provide local information. The idea of using the neutron imaging technique for a hydrogen fuel cell is based on the sensitive response of neutrons to hydrogen-containing compounds such as water. The neutron imaging technique was first used in a PEM fuel cell to determine water distribution in 1999 by Bellows et al. [118]. Subsequently, a few other institutes equipped with neutron sources have explored this technique as an experimental tool to perform in situ non-destructive analysis on an operational PEM fuel cell [112,113,119–121]. For example, Satija et al. [112] used a specially designed neutron imaging setup to pass a neutron beam through the operational fuel cell. The neutron beam was then converted to a light beam that was focused on a CCD camera chip for photos. A real-time radiography consisting of 1000 images at 2-s intervals was used to create a movie that provided an immediate qualitative evaluation of water production, transport and removal throughout the fuel cell. Normalizing the images allowed for the quantitative analysis of the total cell water content, flow field water content and membrane/GDL water content. Despite the various advantages mentioned earlier, the neutron imaging technique has limited application due to the rare availability of radioactive radiation equipment that provides neutron sources.

5.1.2. Measurements of physical indicators

Besides cell voltage losses, water flooding can also cause changes in the characteristic properties of an operating PEM fuel cell. For example, (i) the presence of liquid water in the porous GDL or in the flow field causes the gas flow resistance to rise, which in turn results in an increase in the pressure drop between the inlet and outlet of the fuel cell [103,122]; (ii) water condensation in a local area of a fuel cell leads to a locally lower current density due to water-hindered gas transport; (iii) a locally elevated temperature due to the released enthalpy of the condensing water could result in an uneven local distribution of current density and temperature; and (iv) too much humidification causes flooding, and inadequate humidification leads to a dry membrane, both of which can be reflected in a change in the cell resistance [103]. Based on these relationships between water flooding and the characteristic properties of an operating PEM fuel cell, the measurement of physical indicators has been employed by many researchers as a diagnostic tool to measure the extent of water flooding in an operating fuel cell.

General Motors patented a method and apparatus that was based on pressure drop monitoring for detecting and correcting water flooding in an air-breathing PEM fuel cell [123]. In the embodiment of their invention, if the pressure drop exceeds the predetermined threshold, corrective measures are automatically triggered, such as turning off humidification, reducing gas pressure, increasing gas flow rate, etc. General Motors also patented a method for monitoring the cell resistance in order to avoid the over-humidification that often results in water flooding [124].

He et al. [122] investigated the pressure drop as a function of water flooding of a PEM fuel cell with an interdigitated flow field, under a variety of operating conditions. Due to the strong dependence of the gas permeability of the GDL on liquid water content, the pressure drop between the inlet and outlet, which is inversely proportional to the gas permeability of the GDL, can be correlated with the water saturation level in the GDL. Thus, the pressure drop measurement can be used as an effective diagnostic tool to monitor the liquid water content in the electrode. It can also be used to study the effects of temperature, gas flow rates and GDL properties, such as wetting and water transport characteristics, on the water accumulation and removal rates in the electrodes of PEM fuel cells.

Barbir et al. [103] studied the relationship between pressure drop and cell resistance for a PEM fuel cell stack. They pointed out that, although the increased pressure drop can be a reliable indication of increased water content in the fuel cell, it cannot be used to detect whether the cell is drying out. The reason for this is that in the case of a cell that is drying out, the pressure drop would remain unchanged. However, by combining the pressure drop with the cell resistance measurements, they were able to detect both water flooding and membrane drying in an operational fuel cell stack.

Hakenjos et al. [102] investigated the combined measurement of current and temperature distributions as a diagnostic tool for detection of the flooded areas in the flow field. They focused on the effects of water condensation on the current density and temperature distributions in the flow field. This method was identified as a way to provide experimental data for validating fuel cell simulation and optimizing flow field design.

Stumper et al. [91] developed a diagnostic tool that combined membrane resistance and electrode diffusivity (MRED) measurements with current mapping [125]. Using this diagnostic tool, the distribution of water in the membrane across the active area, and the total amount of liquid water present in the anode or cathode chamber could be determined.

Canut et al. [126] established a detection method that employed the impedance response in conjunction with cell voltage to differentiate the PEM fuel cell stack failures associated with membrane drying and fuel cell flooding.

5.2. Strategies for mitigating water flooding

Optimum cell performance relies strongly on the ability of the fuel cell system to maintain the delicate balance between membrane hydration and avoiding cathode flooding. Achieving this balance has driven persistent research efforts in understanding the role of water in each component of the fuel cell structure, and in developing strategies for proper water management and water flooding mitigation. Ballard (Canada) played a leading role in the 1990s in recognizing water flooding issues and developing various strategies [10,11,127–131]. Nguyen's group at University of Kansas (USA) has recently been very active in areas that relate to the research and development of water management strategies.

The main strategies developed so far for removing cathode water can be summarized as follows.

5.2.1. Flow field design

A long, serpentine oxidant channel layout, along with proper design of the channel dimensions (landing, channel width and depth), has been employed as an effective strategy for removing liquid water. As discussed earlier, the combination of convective force and high-pressure drop along the channel length drives out excess liquid water [107,132]. Recently, Xu et al. developed a new serpentine channel layout by modifying the patterns of conventional serpentine channels to enhance the water removal and mass transfer [133].

In addition to the channel layout strategy, incorporation of special hydrophilic wicking structures into cathode flow channels has also been proposed to redistribute liquid water [134–136]. For example, Ge et al. [136] developed a cathode serpentine flow field mounted with one or two strips of absorbent wicking material (such as PVA sponge, cotton cloth, cotton paper, etc.) to remove liquid water. Using this specially designed flow field, improved water removal was achieved at a current density of 1.2 A cm^{-2}.

Another interesting work related to flow field design was demonstrated by UTC fuel cells [9,137,138] for fuel cell stacks. As shown in Fig. 8, a porous bipolar plate is used as the water transport plate (WTP). The WTP is gas impermeable, preventing gas ingestion into the coolant streams while allowing excess liquid water to be wicked out into the coolant passage network due to the predetermined pressure difference between the gas and the coolant flow field. By using this porous flow field as the water removal tool, the issues associated with liquid water accumulation along the channels of a fuel cell stack were claimed to be minimized and the stack performance penalty for a 20-stack fuel cell eliminated [9].

Other strategies regarding flow field design involve the use of a porous gas distributor plate [137,138], and inclusion of several sequential regions across a plate that have different functions related to water removal and humidification [139].

5.2.2. Anode water removal

A strategy for cathode flooding control, known as "anode water removal", was first developed by Wilkinson et al. at Ballard [10,127]. By appropriate stack design, liquid water accumulated in the cathode can be drawn by a concentration gradient across the membrane to the anode and removed in the fuel stream without causing additional parasitic load. Using this approach, Ballard was able to run fuel cells with an air stoichiometry close to 1.0, without any significant mass transfer losses that could be attributable to cathode flooding. Anode water removal can also be achieved by creating a differential gas pressure between

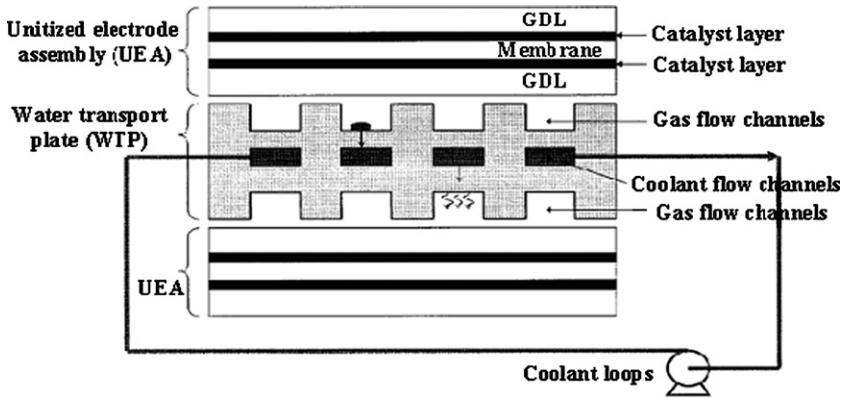

Fig. 8. Within-cell water-exchange system used in UTC Fuel cell [9] (with permission from Wiley Ltd.).

cathode and anode [12,140], that forces liquid water through the membrane from cathode to anode side. However, this high differential pressure requires relatively high operating pressures, which can result in considerable parasitic load, as well as the possibility of membrane rupture in designs that do not adequately support the MEA.

5.2.3. Operating condition control

Manipulation of the operating conditions is a very common strategy to mitigate flooding. These approaches include: increasing cathode gas flow rate well above stoichiometric levels to remove water through evaporation and advection [48,107,127,129,141], flushing the cathode periodically with momentarily high air flow rate [132,141], increasing gas temperature [128], shaking the cell during operation [12], creating a coolant temperature gradient [130], and employing a reactant gas counter-flow operation [131]. This class of strategies often causes significant parasitic losses that are directly linked to pressure, volume flow rate and pressure drop, or that adds to the fuel cell system complexity.

5.2.4. Electro-osmotic pumping

Several groups [48,142–145] have examined the electro-osmotic (EO) pumping technique to mitigate cathode channel flooding. In Buie's experimental setup shown in Fig. 9, two 1.1 mm-thick porous glass EO pumps are placed against the wall

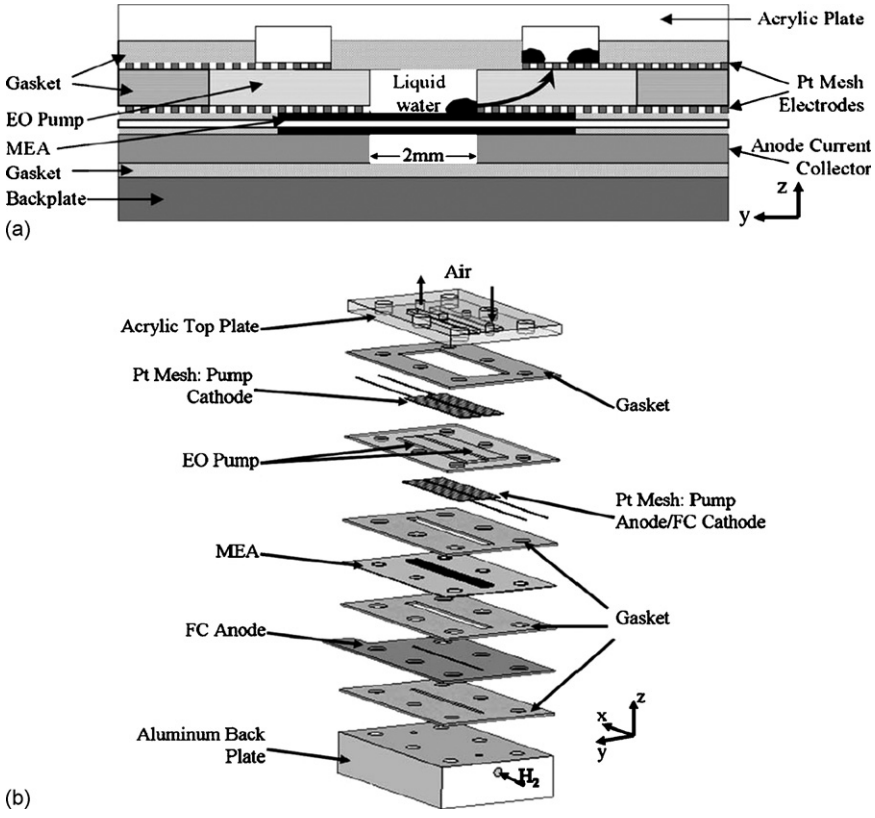

Fig. 9. Schematic of the cross-sectional area (a) and exploded view (b) of a PEM fuel cell design with integrated EO pumping structures [142] (with permission from Elsevier Ltd.).

of the cathode channels. During fuel cell operation, water formed at the cathode is forced out of the GDL by means of hydrophobic forces, and then allowed to transform into water droplets. Liquid water droplets are wicked into the hydrophilic porous glass structure of the EO pump. Once the EO pump structure is adequately saturated with water, EO pumping actively drives water through the porous glass structure into the integrated water reservoirs in the acrylic top plate. It was reported that the EO pumps were able not only to prevent cathode flooding but also to remove water from a flooded cathode to recover the fuel cell, with only a small portion of the fuel cell power, less than 15%, consumed as a parasitic loss.

5.2.5. MEA design

The above four classes of strategies function primarily through system design and engineering, which often adds auxiliary systems to the basic fuel cell system to remove water from the cathode and add significant complexity and cost to the system. A simpler approach for water management through material design and engineering of the components of the MEA is preferred because it does not usually have an associated parasitic load [3,10]. Material design and engineering involves changing the material properties and structures of the GDL and the CCL to function in the presence of liquid water.

Over the last 15 years, several strategies for using materials to address water management in PEM fuel cells have become common practice. Thinner membranes, as thin as 10 μm, have been used to shorten the distance of the water back-diffusion process while, at the same time, to reduce the need for anode humidification and to lower the ionic resistance or ohmic losses through the membrane. However, thinner membranes are often associated with poorer durability and higher gas crossover rates, which has limited the practical membrane thickness to about 25–40 μm for fuel cell applications [146,147].

Optimization of the GDL is another common form of water management strategy, for example, integrating hydrophobic materials (such as PTFE) into the GDL to reject water using a hydrophobic surface, and adding a hydrophobic MPL between the GDL and the catalyst layer to prevent liquid water blockage of reaction zones, both of which have been discussed in detail in Section 3.1.

Modification of the microstructures of the catalyst layer has been a new attempt of material design and engineering to address water management in the PEM fuel cell. The group at University of Kansas (USA) has been active in exploring the creation of a catalyst-layer micro-structure that can withstand higher liquid water saturation levels and can be optimized to handle two-phase transport [3,148]. To reduce the effect of flooding in the CCL, they developed a CCL structure that can provide optimal gas and liquid transport paths to and from the CCL, while maintaining higher electronic and ionic conductivities (Fig. 10). This optimal structure was achieved by first establishing a structure with multiple ionic (Nafion) and electronic (Carbon) interconnected paths for proton and electron transport, and then partially filling the void space with nano-sized hydrophobic particles. The resulting inserted hydrophobic phase provides an independent gas transport path for the reactant gas, which prevents the impairment of

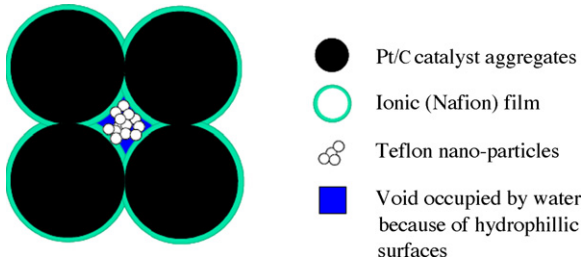

Fig. 10. Distribution of an ideal four-phase (electronic–ionic–gas–liquid) CCL structure [148] (with permission from ECS—The Electrochemical Society).

gas transport by water flooding in the CCL. In comparison to the conventionally made CCL, which consists of a random matrix of catalyst particles, electrolytes and pores, the University of Kansas group's four-phase matrix provides better cell performance at a high current density region where water flooding would normally be occurring.

Another example of using material property design and engineering to address the water management issue is Watanabe et al.'s work on membrane modification. They initially proposed a polymer membrane with porous wicks to directly supply water to the membrane [149] for self-humidification. Later, they described self-humidifying polymer membranes with integrated platinum particles and hygroscopic particles, to produce and store water inside the membrane [150]. Both strategies would require minimal to zero air-side external humidification, thus mitigating the issue of cathode flooding.

Clearly, optimization of the MEA material properties and structures for water removal must be carried out in conjunction with optimization of other requirements, such as good electrical conductivity, liquid permeability, corrosion resistance etc., as well as the operating conditions.

6. Conclusion

Large-scale commercialization of PEM fuel cells calls for lowering cost, increasing durability and optimizing cell performance. PEM fuel cell performance is adversely affected by water flooding that occurs when the liquid water generation rate at the cathode, by electro-osmotic drag and the ORR, exceeds the liquid water removal rate from the cathode by back diffusion to the anode, evaporation, water vapor diffusion and liquid water capillary transport through the GDL. Flooding in the cathode impedes oxygen transport to reaction sites and serves effectively to block the surface area of the catalysts, thereby resulting in a significant, sometimes catastrophic, decrease in cell performance. Water transport and management in PEM fuel cells depends on several variables, such as the structure and properties of the cell components, and the operating conditions, of which the reactant stream humidification, the flow field layout, and the structural and wetting properties of the GDM and MPL are important. Over the last 15 years, extensive research work has been carried out on water flooding, including prediction through numerical modeling, detection by experimental measurements, and mitigation through the design of cell components and the manipulation of operating conditions. Two classes of flooding

mitigation strategies have been developed. One is based on system design and engineering, which is often accompanied by significant parasitic power loss, and the other is based on MEA design and engineering that involves modifying the material and structural properties of the GDL, CCL and membrane to function in the presence of liquid water.

Water management and flooding mitigation are of paramount importance to PEM fuel cell commercialization. Water management and flooding mitigation must be addressed with due consideration to the overall system design, to maintain the overall system simplicity and minimize the system parasitic power loss, thereby decreasing the costs and increasing reliability. Future approaches should focus on the following areas: (i) development of high-temperature PEM fuel cells that can avoid water flooding, due to the absence of liquid water at operation temperatures above 100 °C; (ii) innovative CCL design, such as a thinner catalyst layer for easier water removal, and optimization of the CCL through, for example, structural and hydrophobicity modifications; (iii) new material development, such as a thinner but stronger membrane that not only facilitates easy water removal through the membrane but also improves the reliability of the thin membrane; and (iv) a greater understanding of the fundamental processes of water management and flooding through modeling, especially of the role of the CCL.

Acknowledgements

The authors gratefully acknowledge financial support from the Institute for Fuel Cell Innovation of the National Research Council Canada (NRC-IFCI), Ballard Power Systems and Hydrogenics.

References

[1] K. Jiao, B. Zhou, J. Power Sources 169 (2007) 296.
[2] C. Bao, M. Ouyang, B. Yi, Int. J. Hydrogen Energy 31 (2006) 1879.
[3] T.V. Nguyen, ECS Trans. 3 (2006) 1171.
[4] H.-S. Kim, T.-H. Ha, S.-J. Park, K. Min, M. Kim, Proceedings of the FUELCELL2005 Third International Conference of Fuel Cell Science, Engineering and Technology, 2005, p. 1.
[5] G. Velayutham, J. Kaushik, N. Rajalakshmi, K.S. Dhathathreyan, Fuel Cells 7 (2007) 314.
[6] W. He, Two-phase flow and electrode flooding in PEM fuel cell electrodes, Thesis, University of Kansas, 2003.
[7] D. Natarajan, T. Van Nguyen, J. Power Sources 115 (2003) 66.
[8] C. Song, Y. Tang, J.L. Zhang, J. Zhang, H. Wang, J. Shen, S. McDermid, J. Li, P. Kozak, Electrochim. Acta 52 (2007) 2552.
[9] J.S. Yi, J. Deliang Yang, C. King, AIChE J. 50 (2004) 2594.
[10] D.P. Wilkinson, H.H. Voss, K. Prater, J. Power Sources 49 (1994) 117.
[11] J. St-Pierre, D.P. Wilkinson, S. Knights, M. Bos, J. New Mater. Electrochem. Syst. 3 (2000) 99.
[12] A. Mughal, X. Li, Int. J. Environ. Stud. 63 (2006) 377.
[13] X.G. Yang, N. Burke, C.Y. Wang, K. Tajiri, K. Shinohara, J. Electrochem. Soc. 152 (2005) A759–A766.
[14] J. Zawodzinski, C. Derouin, S. Radzinski, R.J. Sherman, V.T. Smith, T.E. Springer, S. Gottesfeld, J. Electrochem. Soc. 140 (1993) 1041.
[15] T.E. Springer, T.A. Zawodzinski, S. Gottesfeld, J. Electrochem. Soc. 138 (1991) 2334.
[16] G.J.M. Janssen, M.L.J. Overvelde, J. Power Sources 101 (2001) 117.
[17] G. Maggio, V. Recupero, L. Pino, J. Power Sources 101 (2001) 275.
[18] D.L. Wood, J.S. Yi, T.V. Nguyen, Electrochim. Acta 43 (1998) 3795.
[19] M.S. Wilson, C. Zawodzinski, S. Gottesfeld, Proceedings of the Second International Symposium on Proton Conducting Membrane Fuel Cells, vol. II, Pennington, USA, 1998.
[20] C.Y. Wang, Chem. Rev. 104 (2004) 4727.
[21] M.G. Izenson, R.W. Hill, Proceedings of the IMECE2002, ASME International Mechanical Engineering Congress & Exposition, 2002, p. 147.
[22] S. Ge, C.Y. Wang, J. Electrochem. Soc. 154 (2007) B998–B1005.
[23] N. Holmstrom, J. Ihonen, A. Lundblad, G. Lindbergh, Fuel Cells 7 (2007) 306.
[24] M.F. Mathias, J. Roth, J. Fleming, W. Lehnert, W. Vielstich, H.A. Gasteiger, A. Lamm (Eds.), Handbook of Fuel Cells—Fundamentals, Technology and Applications, vol. 3, John Wiley & Sons, New York, 2003 (Chapter 42).
[25] D. Bevers, R. Rogers, M. von Bradke, J. Power Sources 63 (1996) 193.
[26] S. Gamburzev, A.J. Appleby, J. Power Sources 107 (2002) 5.
[27] L.R. Jordan, A.K. Shukla, T. Behrsing, N.R. Avery, B.C. Muddle, M. Forsyth, J. Appl. Electrochem. 30 (2000) 641.
[28] E. Passalacqua, G. Squadrito, F. Lufrano, A. Patti, L. Giorgi, J. Appl. Electrochem. 31 (2001) 449.
[29] N. Djilali, D. Lu, Int. J. Therm. Sci. 41 (2002) 29.
[30] H.K. Atiyeh, K. Karan, B. Peppley, A. Phoenix, E. Halliop, J. Pharoah, J. Power Sources 170 (2007) 111.
[31] J.T. Gostick, M.W. Fowler, M.A. Ioannidis, M.D. Pritzker, Y.M. Volfkovich, A. Sakars, J. Power Sources 156 (2006) 375.
[32] G.G. Park, Y.J. Sohn, T.H. Yang, Y.G. Yoon, W.Y. Lee, C.S. Kim, J. Power Sources 131 (2004) 182.
[33] H.S. Chu, C. Yeh, F. Chen, J. Power Sources 123 (2003) 1.
[34] E. Antolini, R.R. Passos, E.A. Ticianelli, J. Appl. Electrochem. 32 (2002) 383.
[35] S. Litster, G. McLean, J. Power Sources 130 (2004) 61.
[36] J. Ihonen, M. Mikkola, G. Lindbergh, J. Electrochem. Soc. 151 (2004) A1152–A1161.
[37] B. Thoben, A. Siebke, J. New Mater. Electrochem. Syst. 7 (2004) 13.
[38] C. Lim, C.Y. Wang, Electrochim. Acta 49 (2004) 4149.
[39] D. Spernjak, A.K. Prasad, S.G. Advani, J. Power Sources 170 (2007) 334.
[40] P.K. Sinha, Mukherjee S P.P., C.-Y. Wang, J. Mater. Chem. 17 (2007) 3089.
[41] X. Li, I. Sabir, J. Park, J. Power Sources 163 (2007) 933.
[42] T.V. Nguyen, G. Lin, H. Ohn, D. Hussey, D. Jacobson, M. Arif, ECS Trans. 3 (2006) 415.
[43] H. Ohn, T.V. Nguyen, D. Jacobson, D. Hussey, M. Arid, ECS Trans. 1 (2006) 481.
[44] X.G. Yang, F.Y. Zhang, A.L. Lubawy, C.Y. Wang, Electrochem. Solid-State Lett. 7 (2004) A408–A411.
[45] Z.H. Wang, C.Y. Wang, K.S. Chen, J. Power Sources 94 (2001) 40.
[46] H. Dohle, R. Jung, N. Kimiaie, J. Mergel, M. Muller, J. Power Sources 124 (2003) 371.
[47] L. You, H. Liu, Int. J. Heat Mass Transfer 45 (2002) 2277.
[48] K. Tuber, D. Pocza, C. Hebling, J. Power Sources 124 (2003) 403.
[49] S. Shimpalee, U. Beuscher, J.W. Van Zee, Electrochim. Acta 52 (2007) 6748.
[50] M. Prasanna, H.Y. Ha, E.A. Cho, S.-A. Hong, I.-H. Oh, J. Power Sources 131 (2004) 147.
[51] Z. Qi, A. Kaufman, J. Power Sources 109 (2002) 38.
[52] J. Soler, E. Hontanon, L. Daza, J. Power Sources 118 (2003) 172.
[53] T. Hottinen, M. Mikkola, T. Mennola, P. Lund, J. Power Sources 118 (2003) 183.
[54] J.H. Nam, M. Kaviany, Int. J. Heat Mass Transfer 46 (2003) 4595.
[55] J.S. Yi, T. Van Nguyen, J. Electrochem. Soc. 146 (1999) 38.
[56] D. Natarajan, T. Van Nguyen, J. Electrochem. Soc. 148 (2001) A1324–A1335.
[57] U. Pasaogullari, C.Y. Wang, Electrochim. Acta 49 (2004) 4359.
[58] A.Z. Weber, J. Newman, J. Electrochem. Soc. 152 (2005) A677–A688.
[59] U. Pasaogullari, C.Y. Wang, K.S. Chen, J. Electrochem. Soc. 152 (2005) A1574–A1582.
[60] G. Lin, T. Van Nguyen, J. Electrochem. Soc. 153 (2006) A372–A382.

[61] V.A. Paganin, E.A. Ticianelli, E.R. Gonzalez, J. Appl. Electrochem. 26 (1996) 297.
[62] J.M. Song, S.Y. Cha, W.M. Lee, J. Power Sources 94 (2001) 78.
[63] K.H. Choi, D.H. Peck, C.S. Kim, D.R. Shin, T.H. Lee, J. Power Sources 86 (2000) 197.
[64] J. Chen, T. Matsuura, M. Hori, J. Power Sources 131 (2004) 155.
[65] Q. Yan, H. Toghiani, J. Wu, J. Power Sources 158 (2006) 316.
[66] X.L. Wang, H.M. Zhang, J.L. Zhang, H.F. Xu, Z.Q. Tian, J. Chen, H.X. Zhong, Y.M. Liang, B.L. Yi, Electrochim. Acta 51 (2006) 4909.
[67] Y. Cai, J. Hu, H. Ma, B. Yi, H. Zhang, Electrochim. Acta 51 (2006) 6361.
[68] K. Karan, H. Atiyeh, A. Phoenix, E. Halliop, J. Pharoah, B. Peppley, Electrochem. Solid-State Lett. 10 (2007) B34–B38.
[69] M.W. Verbrugge, R.F. Hill, J. Electrochem. Soc. 137 (1990) 886.
[70] M.W. Verbrugge, R.F. Hill, J. Electrochem. Soc. 137 (1990) 1131.
[71] D.M. Bernardi, M.W. Verbrugge, J. Electrochem. Soc. 139 (1992) 2477.
[72] T.E. Springer, M.S. Wilson, S. Gottesfeld, J. Electrochem. Soc. 140 (1993) 3513.
[73] S. Um, C.-Y. Wang, K.S. Chen, J. Electrochem. Soc. 147 (2000) 4485.
[74] L.R. Jordan, A.K. Shukla, T. Behrsing, N.R. Avery, B.C. Muddle, M. Forsyth, J. Power Sources 86 (2000) 250.
[75] L. Giorgi, E. Antolini, A. Pozio, E. Passalacqua, Electrochim. Acta 43 (1998) 3675.
[76] M. Wohr, K. Bolwin, W. Schnurnberger, M. Fischer, W. Neubrand, G. Eigenberger, Int. J. Hydrogen Energy 23 (1998) 213.
[77] T.V. Nguyen, J. Electrochem. Soc. 143 (1996) L103–L105.
[78] X. Liu, H. Guo, C. Ma, J. Power Sources 156 (2006) 267.
[79] W.R. Merida, G. McLean, N. Djilali, J. Power Sources 102 (2001) 178.
[80] D. Xue, Z. Dong, J. Power Sources 76 (1998) 69.
[81] R.S. Gemmen, C.D. Johnson, J. Power Sources 159 (2006) 646.
[82] Z. Qi, A. Kaufman, J. Power Sources 109 (2002) 469.
[83] L. Wang, A. Husar, T. Zhou, H. Liu, Int. J. Hydrogen Energy 28 (2003) 1263.
[84] V. Gurau, H. Liu, S. Kakac, AIChE J. 44 (1998) 2410.
[85] T.F. Fuller, J. Newman, J. Electrochem. Soc. 140 (1993) 1218.
[86] S. Dutta, S. Shimpalee, J.W. Van Zee, J. Appl. Electrochem. 30 (2000) 135.
[87] S. Dutta, S. Shimpalee, J.W. Van Zee, Int. J. Heat Mass Transfer 44 (2001) 2029.
[88] P. Futerko, I.M. Hsing, Electrochim. Acta 45 (2000) 1741.
[89] T.V. Nguyen, R.E. White, J. Electrochem. Soc. 140 (1993) 2178.
[90] J. Allen, ECS Trans. 3 (2006) 1197.
[91] J. Stumper, M. Lohr, S. Hamada, J. Power Sources 143 (2005) 150.
[92] S.Y. Cha, W.M. Lee, J. Electrochem. Soc. 146 (1999) 4055.
[93] R. O'Hayre, S.J. Lee, S.W. Cha, F. Prinz, J. Power Sources 109 (2002) 483.
[94] M. Eikerling, A.A. Kornyshev, J. Electroanal. Chem. 453 (1998) 89.
[95] I.E. Baranov, S.A. Grigoriev, D. Ylitalo, V.N. Fateev, I.I. Nikolaev, Int. J. Hydrogen Energy 31 (2006) 203.
[96] J.J. Baschuk, X. Li, J. Power Sources 86 (2000) 181.
[97] S. Maharudrayya, S. Jayanti, A.P. Deshpande, Proceedings of the FUELCELL2005, Third International Conference of Fuel Cell Science, Engineering and Technology, 2005, p. 1.
[98] P.C. Sui, Med Djilali, J. Fuel Cell Sci. Technol. 2 (2005) 149.
[99] D.M. Bernardi, J. Electrochem. Soc. 137 (1990) 3344.
[100] P. Berg, K. Promislow, J.S. Pierre, J. Stumper, B. Wetton, J. Electrochem. Soc. 151 (2004) A341–A353.
[101] W.K. Lee, J.W. Van Zee, Proc. ASME, Heat Transfer Div. 1 (1999) 359.
[102] A. Hakenjos, H. Muenter, U. Wittstadt, C. Hebling, J. Power Sources 131 (2004) 213.
[103] F. Barbir, H. Gorgun, X. Wang, J. Power Sources 141 (2005) 96.
[104] D. Song, Q. Wang, Z.S. Liu, C. Huang, J. Power Sources 159 (2006) 928.
[105] W. He, J.S. Yi, T. Van Nguyen, AIChE J. 46 (2000) 2053.
[106] G. Lin, W. He, T. Van Nguyen, J. Electrochem. Soc. 151 (2004) A1999–A2006.
[107] U. Pasaogullari, C.Y. Wang, J. Electrochem. Soc. 152 (2005) A380–A390.
[108] A.Z. Weber, J. Newman, Chem. Rev. 104 (2004) 4679.
[109] W.Q. Tao, C.H. Min, X.L. Liu, Y.L. He, B.H. Yin, W. Jiang, J. Power Sources 160 (2006) 359.
[110] A. Biyikoglu, Int. J. Hydrogen Energy 30 (2005) 1181.
[111] F.Y. Zhang, X.G. Yang, C.Y. Wang, J. Electrochem. Soc. 153 (2006) A225–A232.
[112] R. Satija, D.L. Jacobson, M. Arif, S.A. Werner, J. Power Sources 129 (2004) 238.
[113] N. Pekula, K. Heller, P.A. Chuang, A. Turhan, M.M. Mench, J.S. Brenizer, K. Unlu, Nucl. Instrum. Methods Phys. Res. Sect. A: Accel. Spectrom. Detect. Assoc. Equip. 542 (2005) 134.
[114] S. Tsushima, T. Nanjo, K. Nishida, S. Hirai, ECS Trans. 1 (2006) 199.
[115] S. Tsushima, K. Teranishi, S. Hirai, Electrochem. Solid-State Lett. 7 (2004) A269–A272.
[116] P.K. Sinha, P. Halleck, C. Wang, Electrochem. Solid-State Lett. 9 (2006) A344–A348.
[117] A. Bazylak, D. Sinton, Z.S. Liu, N. Djilali, J. Power Sources 163 (2007) 784.
[118] R.J. Bellows, M.Y. Lin, M. Arif, A.K. Thompson, D. Jacobson, J. Electrochem. Soc. 146 (1999) 1099.
[119] J.J. Kowal, A. Turhan, K. Heller, J. Brenizer, M.M. Mench, J. Electrochem. Soc. 153 (2006) A1971–A1978.
[120] M.A. Hickner, N.P. Siegel, K.S. Chen, D.N. McBrayer, D.S. Hussey, D.L. Jacobson, M. Arif, J. Electrochem. Soc. 153 (2006) A902–A908.
[121] T.A. Trabold, J.P. Owejan, D.L. Jacobson, M. Arif, P.R. Huffman, Int. J. Heat Mass Transfer 49 (2006) 4712.
[122] W. He, G. Lin, T. Van Nguyen, AIChE J. 49 (2003) 3221.
[123] A.D. Bosco, M.H. Fronk, US Patent Ch.6,103,409 (2000).
[124] M.F. Mathias, S.A. Grot, US Patent Ch.6,376,111 (2002).
[125] J. Stumper, S.A. Campbell, D.P. Wilkinson, M.C. Johnson, M. Davis, Electrochim. Acta 43 (1998) 3773.
[126] J.M.L. Canut, R.M. Abouatallah, D.A. Harrington, J. Electrochem. Soc. 153 (2006) A857–A864.
[127] H.H. Voss, D.P. Wilkinson, P.G. Pickup, M.C. Johnson, V. Basura, Electrochim. Acta 40 (1995) 321.
[128] J. St-Pierre, D.P. Wilkinson, H. Voss, R. Pow, New Materials for Fuel Cell and Modern Battery Systems II: Proceedings of the Second International Symposium on New Materials for Fuel Cell and Modern Battery Systems, Montreal, Canada, 1997, p. 318.
[129] H.H. Voss, D.P. Wilkinson, D.S. Watkins, US Ch.5,441,819 (1995).
[130] N.J. Fletcher, C.Y. Chow, E.G. Pow, B.M. Wozniczka, H.H. Voss, G. Hornburg, D.P. Wilkinson, US Patent Ch.5,547,776 (1996).
[131] D.P. Wilkinson, H.H. Voss, N.J. Fletcher, M.C. Johnson, E.G. Pow, US Patent Ch.5,773,160 (1998).
[132] M.W. Knobbe, W. He, P.Y. Chong, T.V. Nguyen, J. Power Sources 138 (2004) 94.
[133] C. Xu, T.S. Zhao, Electrochem. Commun. 9 (2007) 497.
[134] S. Ge, X. Li, I.M. Hsing, Electrochim. Acta 50 (2005) 1909.
[135] R. Eckl, W. Zehtner, C. Leu, U. Wagner, J. Power Sources 138 (2004) 137.
[136] S.H. Ge, X.G. Li, I.M. Hsing, J. Electrochem. Soc. 151 (2004) B523–B528.
[137] S. Miachon, P. Aldebert, J. Power Sources 56 (1995) 31.
[138] A.P. Meyer, G.W. Scheffler, P.R. Margiott, US Patent Ch.5,503,994 (1996).
[139] N.E. Vanderborgh, J.C. Hestrom, US Patent Ch.4,973,530 (1990).
[140] J.S. Yi, T.V. Nguyen, J. Electrochem. Soc. 145 (1998) 1149.
[141] T. Van Nguyen, M.W. Knobbe, J. Power Sources 114 (2003) 70.
[142] C.R. Buie, J.D. Posner, T. Fabian, S.W. Cha, D. Kim, F.B. Prinz, J.K. Eaton, J.G. Santiago, J. Power Sources 161 (2006) 191.
[143] S. Litster, C.R. Buie, T. Fabian, J.K. Eaton, J.G. Santiago, J. Electrochem. Soc. 154 (2007) B1049–B1058.
[144] D.J.L. Brett, S. Atkins, N.P. Brandon, V. Vesovic, N. Vasileiadis, A. Kucernak, Electrochem. Solid-State Lett. 6 (2003) A63–A66.
[145] D.J.L. Brett, S. Atkins, N.P. Brandon, V. Vesovic, N. Vasileiadis, A.R. Kucernak, Electrochem. Commun. 3 (2001) 628.

[146] T.J.P. Freire, E.R. Gonzalez, J. Electroanal. Chem. 503 (2001) 57.
[147] D.H. Peck, Y.G. Chun, C.S. Kim, D.H. Jung, d.R. Shin, J. New Mater. Electrochem. Syst. 2 (1999) 121.
[148] T.V. Nguyen, D. Natarajan, R. Jain, ECS Trans. 1 (2006) 501.
[149] M. Watanabe, Y. Satoh, C. Shimura, J. Electrochem. Soc. 140 (1993) 3190.
[150] M. Watanabe, H. Uchida, Y. Seki, M. Emori, P. Stonehart, J. Electrochem. Soc. 143 (1996) 3847.